MOJAVE: MONITORING OF JETS IN ACTIVE GALACTIC NUCLEI WITH VLBA EXPERIMENTS. V. MULTI-EPOCH VLBA IMAGES

M. L. Lister[1], H. D. Aller[2], M. F. Aller[2], M. H. Cohen[3], D. C. Homan[4], M. Kadler[5,6,7,8], K. I. Kellermann[9], Y. Y. Kovalev[10,11], E. Ros[10], T. Savolainen[10], J. A. Zensus[10], AND R. C. Vermeulen[12]

[1] Department of Physics, Purdue University, 525 Northwestern Avenue, West Lafayette, IN 47907, USA; mlister@purdue.edu
[2] Department of Astronomy, University of Michigan, 817 Denison Building, Ann Arbor, MI 48109-1042, USA; haller@umich.edu, mfa@umich.edu
[3] Department of Astronomy, California Institute of Technology, Mail Stop 105-24, Pasadena, CA 91125, USA; mhc@astro.caltech.edu
[4] Department of Physics and Astronomy, Denison University, Granville, OH 43023, USA; homand@denison.edu
[5] Dr. Remeis-Sternwarte Bamberg, Universität Erlangen-Nürnberg, Sternwartstrasse 7, 96049 Bamberg, Germany
[6] Erlangen Centre for Astroparticle Physics, Erwin-Rommel Str. 1, 91058 Erlangen, Germany
[7] CRESST/NASA Goddard Space Flight Center, Greenbelt, MD 20771, USA
[8] Universities Space Research Association, 10211 Wincopin Circle, Suite 500, Columbia, MD 21044, USA; matthias.kadler@sternwarte.uni-erlangen.de
[9] National Radio Astronomy Observatory, 520 Edgemont Road, Charlottesville, VA 22903-2475, USA; kkellerm@nrao.edu
[10] Max-Planck-Institut für Radioastronomie, Auf dem Hügel 69, D-53121 Bonn, Germany; ros@mpifr-bonn.mpg.de, tsavolainen@mpifr-bonn.mpg.de, azensus@mpifr-bonn.mpg.de
[11] Astro Space Center of Lebedev Physical Institute, Profsoyuznaya 84/32, 117997 Moscow, Russia; ykovalev@mpifr-bonn.mpg.de
[12] ASTRON, Postbus 2, NL-7990 AA Dwingeloo, Netherlands; rvermeulen@astron.nl

ABSTRACT

We present images from a long-term program (MOJAVE: Monitoring of Jets in active galactic nuclei (AGNs) with VLBA Experiments) to survey the structure and evolution of parsec-scale jet phenomena associated with bright radio-loud active galaxies in the northern sky. The observations consist of 2424 15 GHz Very Long Baseline Array (VLBA) images of a complete flux-density-limited sample of 135 AGNs above declination $-20°$, spanning the period 1994 August to 2007 September. These data were acquired as part of the MOJAVE and 2 cm Survey programs, and from the VLBA archive. The sample-selection criteria are based on multi-epoch parsec-scale (VLBA) flux density, and heavily favor highly variable and compact blazars. The sample includes nearly all the most prominent blazars in the northern sky, and is well suited for statistical analysis and comparison with studies at other wavelengths. Our multi-epoch and stacked-epoch images show 94% of the sample to have apparent one-sided jet morphologies, most likely due to the effects of relativistic beaming. Of the remaining sources, five have two-sided parsec-scale jets, and three are effectively unresolved by the VLBA at 15 GHz, with essentially all of the flux density contained within a few tenths of a milliarcsecond.

Key words: BL Lacertae objects: general – galaxies: active – galaxies: jets – quasars: general – radio continuum: galaxies – surveys

Online-only material: figure sets, machine-readable and VO tables

1. INTRODUCTION

High angular resolution studies of the kinematics of active galactic nucleus (AGN) jets over many years have led to a better understanding of the process of acceleration and collimation of the relativistic jets associated with the ejection of relativistic plasma from a central supermassive black hole. Early observations were made with ad hoc arrays comprised of relatively few antennas and focused on a few relatively strong and fast superluminal sources (e.g., Cohen et al. 1975; Shaffer et al. 1975; Schilizzi et al. 1975). In these studies, it was difficult to trace details of the jet outflow due to limited temporal and interferometric coverage of the arrays, which consisted of existing antennas with differing instrumental characteristics. Moreover, by concentrating on only the fastest or most interesting sources, (e.g., Cohen et al. 1977; Zensus et al. 1995), the kinematic results did not reflect the full range of speeds seen in the overall population. With the start of Very Long Baseline Array (VLBA) operations in the mid-1990s, we were able to obtain a reasonably uniform set of multi-epoch 15 GHz (2 cm) observations on 132 AGNs (Kellermann et al. 1998; Zensus et al. 2002) which covered the period 1994–2002. From these data, we were able to discuss the statistical properties of AGN jets (Kellermann et al. 2004; Kovalev et al. 2005; Homan et al.

2006), including the intrinsic properties of the parent population (Cohen et al. 2007) and the detailed nature of a few sources of particular interest (Homan et al. 2003; Vermeulen et al. 2003; Lister et al. 2003; Kadler et al. 2008; Kovalev et al. 2007).

Although these studies included most known "flat spectrum" ($\alpha > -0.5$, where $S_\nu \propto \nu^\alpha$) radio sources with total flux density above well defined limits, they included or excluded some sources because of the contribution of extended emission, errors in the measured spectral index, and/or spectral curvature. As described in Paper I of this series (Lister & Homan 2005), our new Monitoring of Jets in Active Galactic Nuclei with VLBA Experiments (MOJAVE) sample includes all sources with measured total VLBA flux density at 15 GHz greater than a defined flux density at any epoch during the period 1994.0–2004.0. For the 96 sources in common with the studies of Kellermann et al. (1998) and Zensus et al. (2002), the timescale for determining the speed and possible accelerations or decelerations is now extended from 7 to 13 years. Lister & Homan (2005) give more details of the sample definition and also discuss the single-epoch linear polarization properties of the MOJAVE sample, while Homan & Lister (2006) discuss the circular polarization properties (Paper II).

The MOJAVE/2 cm Survey program is among the largest multi-epoch AGN VLBI surveys carried out to date, and is

complemented by several programs at other wavelengths. These include the 5 GHz Caltech–Jodrell Flat-Spectrum Survey (Britzen et al. 2007, 2008), the 2 & 8 GHz Radio Reference Frame program (Piner et al. 2007), and the 43 GHz Boston University AGN monitoring program (Jorstad et al. 2007). Each of these programs offers various trade-offs in terms of sample size, angular resolution, and image sensitivity. Shorter wavelength studies, such as the Boston University program, provide better angular resolution than at 15 GHz, but the sensitivity is poorer, jet features fade faster, and the impact of tropospheric conditions is more severe. Thus, short wavelength observations need to be more frequent, and consequently must focus on much smaller samples of extremely bright sources. Longer wavelength studies have better surface brightness sensitivity and so can trace the jet motions out to greater distances, but at the expense of degraded angular resolution.

This paper is the fifth in a series describing the results of the MOJAVE program, with the most recent ones discussing the kiloparsec-scale jet properties (Cooper et al. 2007; Paper III) and parent luminosity function (Cara & Lister 2008; Paper IV) of the sample. Here, we present a complete set of 15 GHz VLBA images of the flux-density-limited MOJAVE sample of 135 compact extragalactic radio jets obtained during the period 1994 August to 2007 September. The overall layout of the paper is as follows: in Section 2 we discuss the sample definition and selection criteria, in Section 3 we discuss our observational program and data reduction method, and in Section 4 we summarize the overall parsec-scale morphological properties of the AGN jets and describe our current monitoring program. In subsequent papers, we will discuss their kinematic properties, overall demographics, and polarization properties.

2. SAMPLE DEFINITION

In Paper I, we described our selection criteria for the MOJAVE sample, which is based on compact radio flux density in order to provide the best comparison with Monte Carlo samples of relativistically beamed jets (e.g., Lister & Marscher 1997). By using the milliarcsecond scale (VLBA) 15 GHz flux density rather than total flux density as the selection criterion, we were effectively able to exclude any contribution from large-scale emission, leaving a sample consisting almost entirely of radio-loud AGNs with relativistic jets pointed close to the line of sight (LOS; i.e., blazars). The only exceptions were a handful of nearby radio galaxies and peaked-spectrum sources whose jet axes probably lie much closer to the plane of the sky.

The MOJAVE selection criteria resemble those of the original VLBA 2 cm Survey of Kellermann et al. (1998), and are defined as follows:

(1) J2000 declination $\geqslant -20°$;
(2) Galactic latitude $|b| \geqslant 2°.5$; and
(3) total 15 GHz VLBA flux density of at least 1.5 Jy ($\geqslant 2$ Jy for sources below the celestial equator) *at any epoch* during the period 1994.0–2004.0.

Because of the highly variable nature of strong, compact AGNs, we did not limit the flux density criterion to a single fixed epoch. Doing so would have excluded many highly variable sources from the sample, and would subsequently reduce the robustness of statistical tests on source properties. Including the variable AGN also provides a more complete sample for comparisons with AGN surveys at other wavelengths, such as the 3rd EGRET (Hartman et al. 1999) and upcoming Fermi

(Thompson 2004) gamma-ray catalogs. The higher flux density limit for the southern sources was chosen since the VLBA has reduced hour angle coverage for this region of the sky and consequently poorer imaging capability.

We note that for several sources in our sample, we did not have any 15 GHz VLBA measurements that formally met our flux density criterion. However, we were able to infer their VLBA flux density at other epochs by using an extensive database of flux density measurements from the UMRAO and RATAN telescopes spanning 1994.0–2004.0 (e.g., Kovalev et al. 1999; Aller et al. 1992). An important step in this method was to determine the amount of extended (non-VLBA) flux density in each source using near-simultaneous UMRAO/VLBA measurements made at multiple epochs.

In Paper I, we originally identified a total of 133 AGNs that satisfied these criteria. In processing additional archival VLBA epochs for the current paper, we have subsequently identified two more sources (0838+133 and 1807+698) which met our selection criteria, bringing the total number up to 135 AGNs. One additional source, 1150+497, appears to have possibly met the MOJAVE criteria based on the interpolation of single-dish RATAN radio observations in 2003 August, however, we did not obtain any 15 GHz VLBA epochs on this source prior to 2008. This source is now currently in our extended monitoring program (see Section 4.3). We believe the overall completeness of the MOJAVE survey to be high, with few sources missed, because of our large preselection candidate list (see Paper I) and the extensive flux density database that was available from the VLBA, RATAN, and UMRAO facilities.

We list the general properties of the MOJAVE sources in Table 1. The redshifts are gathered from the literature, and are currently only 93% complete, mainly because of the featureless spectra of several BL Lacs in the sample. We list the nature of the optical counterpart from Véron-Cetty & Véron (2006) for each AGN in Column (6), except as noted in Table 1. At the present time, only four sources (0446+113, 0648−165, 1213−172, and 2021+317) lack published optical counterparts.

The MOJAVE sample is dominated by quasars, with the weak-lined BL Lacertae objects and radio galaxies making up 16% and 6% of the sample, respectively. Véron-Cetty & Véron (2006) have recently reclassified as quasars some BL Lac objects that have occasionally displayed emission lines slightly wider than the nominal 5 Å equivalent width limit (Stickel et al. 1991). Since these are still much narrower than those typically found in quasars, we have chosen to list the previous BL Lac classifications for these objects, and have indicated these with flags in Table 1. The classifications of the radio spectral shape given in Column (7) are described by Kellermann et al. (2004). The MOJAVE sample is heavily dominated by blazars with flat overall radio spectra, which we define as a spectral index α flatter than -0.5 at any frequency between 0.6 and 22 GHz. The five steep-spectrum sources in the sample have strong extended emission on arcsecond scales that dominates the integrated spectrum, but their parsec-scale emission still met our selection criteria. Two of the latter AGNs (1458+718 and 1823+487) are frequently referred to as compact steep-spectrum sources in the literature. All of the sources originally described in Paper I as peaked spectrum, with the exception of 0742+103, have subsequently turned out to have variable radio spectra and are therefore no longer considered as stable peaked-spectrum sources (e.g., Torniainen et al. 2005).

Table 1
The Complete Flux-Limited MOJAVE AGN Sample

Source (1)	Alias (2)	R.A. (3)	Decl. (4)	N (5)	Opt. Cl. (6)	Radio (7)	z (8)	Reference for z (9)
0003−066	NRAO 005	$00^h06^m13\!\!.\!8929$	$-06°23'35\!\!.\!3353$	19	B	F	0.347	Stickel et al. (1989)
0007+106	III Zw 2	$00^h10^m31\!\!.\!0059$	$+10°58'29\!\!.\!5044$	15	G	F	0.0893	Sargent (1970)
0016+731	⋯	$00^h19^m45\!\!.\!7864$	$+73°27'30\!\!.\!0175$	12	Q	F	1.781	Lawrence et al. (1996)
0048−097	⋯	$00^h50^m41\!\!.\!3174$	$-09°29'05\!\!.\!2103$	14	B	F	⋯	⋯
0059+581	⋯	$01^h02^m45\!\!.\!7624$	$+58°24'11\!\!.\!1366$	13	Q[d]	F	0.644	Sowards-Emmerd et al. (2005)
0106+013	⋯	$01^h08^m38\!\!.\!7711$	$+01°35'00\!\!.\!3173$	15	Q	F	2.099	Hewett et al. (1995)
0109+224	⋯	$01^h12^m05\!\!.\!8247$	$+22°44'38\!\!.\!7864$	9	B	F	0.265	Healey et al. (2008)
0119+115	⋯	$01^h21^m41\!\!.\!5950$	$+11°49'50\!\!.\!4131$	11	Q	F	0.570	Stickel et al. (1994)
0133+476	DA 55	$01^h36^m58\!\!.\!5948$	$+47°51'29\!\!.\!1001$	25	Q	F	0.859	Lawrence et al. (1996)
0202+149	4C +15.05	$02^h04^m50\!\!.\!4139$	$+15°14'11\!\!.\!0437$	13	Q[c]	F	0.405	Perlman et al. (1998)
0202+319	⋯	$02^h05^m04\!\!.\!9254$	$+32°12'30\!\!.\!0955$	12	Q	F	1.466	Burbidge (1970)
0212+735	⋯	$02^h17^m30\!\!.\!8134$	$+73°49'32\!\!.\!6218$	14	Q	F	2.367	Lawrence et al. (1996)
0215+015	OD 026	$02^h17^m48\!\!.\!9548$	$+01°44'49\!\!.\!6991$	17	Q	F	1.715	Boisse & Bergeron (1988)
0224+671	4C +67.05	$02^h28^m50\!\!.\!0515$	$+67°21'03\!\!.\!0294$	8	Q[d]	F	0.523	Sowards-Emmerd et al. (2005)
0234+285	CTD 20	$02^h37^m52\!\!.\!4057$	$+28°48'08\!\!.\!9901$	16	Q	F	1.207	Schmidt (1977)
0235+164	⋯	$02^h38^m38\!\!.\!9301$	$+16°36'59\!\!.\!2746$	36	B[a]	F	0.940	Cohen et al. (1987)
0238−084	NGC 1052	$02^h41^m04\!\!.\!7985$	$-08°15'20\!\!.\!7518$	30	G	F	0.005037	Denicoló et al. (2005)
0300+470	4C +47.08	$03^h03^m35\!\!.\!2422$	$+47°16'16\!\!.\!2755$	11	B	F	⋯	⋯
0316+413	3C 84	$03^h19^m48\!\!.\!1601$	$+41°30'42\!\!.\!1048$	22	G	F	0.0176	Strauss et al. (1992)
0333+321	NRAO 140	$03^h36^m30\!\!.\!1076$	$+32°18'29\!\!.\!3423$	18	Q	F	1.259	Steidel & Sargent (1991)
0336−019	CTA 26	$03^h39^m30\!\!.\!9378$	$-01°46'35\!\!.\!8041$	16	Q	F	0.852	Wills & Lynds (1978)
0403−132	⋯	$04^h05^m34\!\!.\!0034$	$-13°08'13\!\!.\!6907$	10	Q	F	0.571	Marziani et al. (1996)
0415+379	3C 111	$04^h18^m21\!\!.\!2772$	$+38°01'35\!\!.\!8001$	24	G	S	0.0491	Eracleous & Halpern (2004)
0420−014	⋯	$04^h23^m15\!\!.\!8007$	$-01°20'33\!\!.\!0654$	43	Q	F	0.914	Wills & Lynds (1978)
0422+004	⋯	$04^h24^m46\!\!.\!8421$	$+00°36'06\!\!.\!3293$	8	B	F	⋯	⋯
0430+052	3C 120	$04^h33^m11\!\!.\!0955$	$+05°21'15\!\!.\!6192$	43	G	F	0.033	Michel & Huchra (1988)
0446+112	⋯	$04^h49^m07\!\!.\!6711$	$+11°21'28\!\!.\!5965$	9	U[b]	F	⋯	⋯
0458−020	⋯	$05^h01^m12\!\!.\!8099$	$-01°59'14\!\!.\!2562$	10	Q	F	2.286	Strittmatter et al. (1974)
0528+134	⋯	$05^h30^m56\!\!.\!4167$	$+13°31'55\!\!.\!1496$	24	Q	F	2.070	Hunter et al. (1993)
0529+075	⋯	$05^h32^m38\!\!.\!9985$	$+07°32'43\!\!.\!3451$	6	Q[d]	F	1.254	Sowards-Emmerd et al. (2005)
0529+483	⋯	$05^h33^m15\!\!.\!8658$	$+48°22'52\!\!.\!8079$	10	Q	F	1.162	Halpern et al. (2003)
0552+398	DA 193	$05^h55^m30\!\!.\!8056$	$+39°48'49\!\!.\!1650$	28	Q	F	2.363	McIntosh et al. (1999)
0605−085	OC −010	$06^h07^m59\!\!.\!6992$	$-08°34'49\!\!.\!9782$	15	Q	F	0.872	Stickel et al. (1993)
0607−157	⋯	$06^h09^m40\!\!.\!9495$	$-15°42'40\!\!.\!6726$	20	Q	F	0.324	Hunstead et al. (1978)
0642+449	OH 471	$06^h46^m32\!\!.\!0260$	$+44°51'16\!\!.\!5901$	10	Q	F	3.396	Osmer et al. (1994)
0648−165	⋯	$06^h50^m24\!\!.\!5819$	$-16°37'39\!\!.\!7253$	6	U[d]	F	⋯	⋯
0716+714	⋯	$07^h21^m53\!\!.\!4485$	$+71°20'36\!\!.\!3634$	26	B	F	0.310	Nilsson et al. (2008)
0727−115	⋯	$07^h30^m19\!\!.\!1125$	$-11°41'12\!\!.\!6005$	11	Q	F	1.591	Zensus et al. (2002)
0730+504	⋯	$07^h33^m52\!\!.\!5206$	$+50°22'09\!\!.\!0621$	7	Q	F	0.720	Henstock et al. (1997)
0735+178	OI 158	$07^h38^m07\!\!.\!3937$	$+17°42'18\!\!.\!9982$	24	B	F	⋯	⋯
0736+017	OI 061	$07^h39^m18\!\!.\!0339$	$+01°37'04\!\!.\!6178$	14	Q	F	0.191	Lynds (1967)
0738+313	OI 363	$07^h41^m10\!\!.\!7033$	$+31°12'00\!\!.\!2291$	17	Q	F	0.631	Abazajian et al. (2004)
0742+103	⋯	$07^h45^m33\!\!.\!0595$	$+10°11'12\!\!.\!6923$	15	Q[d]	P	2.624	Best et al. (2003)
0748+126	⋯	$07^h50^m52\!\!.\!0457$	$+12°31'04\!\!.\!8282$	16	Q	F	0.889	Peterson et al. (1979)
0754+100	⋯	$07^h57^m06\!\!.\!6429$	$+09°56'34\!\!.\!8525$	16	B	F	0.266	Carangelo et al. (2003)
0804+499	⋯	$08^h08^m39\!\!.\!6663$	$+49°50'36\!\!.\!5304$	12	Q	F	1.436	Adelman-McCarthy et al. (2006)
0805−077	⋯	$08^h08^m15\!\!.\!5360$	$-07°51'09\!\!.\!8864$	7	Q	F	1.837	White et al. (1988)
0808+019	⋯	$08^h11^m26\!\!.\!7073$	$+01°46'52\!\!.\!2202$	11	B	F	1.148	Sbarufatti et al. (2005)
0814+425	OJ 425	$08^h18^m15\!\!.\!9996$	$+42°22'45\!\!.\!4149$	15	B	F	0.245	Britzen et al. (2008)
0823+033	⋯	$08^h25^m50\!\!.\!3384$	$+03°09'24\!\!.\!5201$	22	B	F	0.506	Stickel et al. (1993)
0827+243	OJ 248	$08^h30^m52\!\!.\!0862$	$+24°10'59\!\!.\!8204$	19	Q	F	0.940	Adelman-McCarthy et al. (2007)
0829+046	OJ 049	$08^h31^m48\!\!.\!8770$	$+04°29'39\!\!.\!0859$	26	B	F	0.174	Abazajian et al. (2005)
0836+710	4C 71.07	$08^h41^m24\!\!.\!3653$	$+70°53'42\!\!.\!1730$	13	Q	F	2.218	McIntosh et al. (1999)
0838+133	3C 207	$08^h40^m47\!\!.\!5884$	$+13°12'23\!\!.\!5641$	16	Q	F	0.681	Marziani et al. (1996)
0851+202	OJ 287	$08^h54^m48\!\!.\!8749$	$+20°06'30\!\!.\!6409$	69	B	F	0.306	Stickel et al. (1989)
0906+015	4C +01.24	$09^h09^m10\!\!.\!0916$	$+01°21'35\!\!.\!6180$	12	Q	F	1.024	Abazajian et al. (2004)
0917+624	⋯	$09^h21^m36\!\!.\!2311$	$+62°15'52\!\!.\!1804$	13	Q	F	1.446	Stickel & Kühr (1993b)
0923+392	4C +39.25	$09^h27^m03\!\!.\!0139$	$+39°02'20\!\!.\!8519$	26	Q	F	0.695	Abazajian et al. (2005)
0945+408	4C +40.24	$09^h48^m55\!\!.\!3382$	$+40°39'44\!\!.\!5869$	13	Q	F	1.249	Abazajian et al. (2005)
0955+476	⋯	$09^h58^m19\!\!.\!6716$	$+47°25'07\!\!.\!8424$	7	Q	F	1.882	Abazajian et al. (2004)
1036+054	⋯	$10^h38^m46\!\!.\!7799$	$+05°12'29\!\!.\!0867$	7	Q[d]	F	0.473	Healey et al. (2008)
1038+064	4C +06.41	$10^h41^m17\!\!.\!1625$	$+06°10'16\!\!.\!9235$	8	Q	F	1.265	Steidel & Sargent (1991)
1045−188	⋯	$10^h48^m06\!\!.\!6206$	$-19°09'35\!\!.\!7268$	6	Q	F	0.595	Stickel et al. (1993)

Table 1
(Continued)

Source (1)	Alias (2)	R.A. (3)	Decl. (4)	N (5)	Opt. Cl. (6)	Radio (7)	z (8)	Reference for z (9)
1055+018	4C +01.28	10^{h}58^{m}29^s.6052	+01°33′58″.8237	27	Q	F	0.890	Croom et al. (2004)
1124−186	⋯	11^{h}27^{m}04^s.3925	−18°57′17″.4417	7	Q	F	1.048	Drinkwater et al. (1997)
1127−145	⋯	11^{h}30^{m}07^s.0526	−14°49′27″.3882	16	Q	F	1.184	Wilkes (1986)
1150+812	⋯	11^{h}53^{m}12^s.4992	+80°58′29″.1546	11	Q	F	1.250	Eckart et al. (1986)
1156+295	4C +29.45	11^{h}59^{m}31^s.8339	+29°14′43″.8269	30	Q	F	0.729	Aldcroft et al. (1994)
1213−172	⋯	12^{h}15^{m}46^s.7518	−17°31′45″.4029	7	U[d]	F	⋯	⋯
1219+044	⋯	12^{h}22^{m}22^s.5496	+04°13′15″.7761	6	Q	F	0.965	Wilkes (1986)
1222+216	⋯	12^{h}24^{m}54^s.4584	+21°22′46″.3887	16	Q	F	0.432	Osterbrock & Pogge (1987)
1226+023	3C 273	12^{h}29^{m}06^s.6997	+02°03′08″.5981	54	Q	F	0.158	Strauss et al. (1992)
1228+126	M87	12^{h}30^{m}49^s.4234	+12°23′28″.0438	25	G	S	0.00436	Smith et al. (2000)
1253−055	3C 279	12^{h}56^{m}11^s.1666	−05°47′21″.5247	89	Q	F	0.536	Marziani et al. (1996)
1308+326	⋯	13^{h}10^{m}28^s.6639	+32°20′43″.7829	44	Q	F	0.997	Tytler & Fan (1992)
1324+224	⋯	13^{h}27^{m}00^s.8613	+22°10′50″.1630	8	Q	F	1.400	Hook et al. (1996)
1334−127	⋯	13^{h}37^{m}39^s.7828	−12°57′24″.6933	16	Q	F	0.539	Stickel et al. (1993)
1413+135	⋯	14^{h}15^{m}58^s.8175	+13°20′23″.7128	18	B	F	0.247	Wiklind & Combes (1997)
1417+385	⋯	14^{h}19^{m}46^s.6138	+38°21′48″.4751	6	Q	F	1.831	Adelman-McCarthy et al. (2006)
1458+718	3C 309.1	14^{h}59^{m}07^s.5839	+71°40′19″.8665	9	Q	S[e]	0.904	Veron-Cetty & Veron (1989)
1502+106	4C +10.39	15^{h}04^{m}24^s.9798	+10°29′39″.1986	11	Q	F	1.839	Akiyama et al. (2003)
1504−166	⋯	15^{h}07^{m}04^s.7870	−16°52′30″.2670	7	Q	F	0.876	Hunstead et al. (1978)
1510−089	⋯	15^{h}12^{m}50^s.5329	−09°05′59″.8297	31	Q	F	0.360	Thompson et al. (1990)
1538+149	4C +14.60	15^{h}40^{m}49^s.4915	+14°47′45″.8848	13	B[a]	F	0.605	Stickel et al. (1993)
1546+027	⋯	15^{h}49^{m}29^s.4368	+02°37′01″.1634	15	Q	F	0.414	Abazajian et al. (2004)
1548+056	4C +05.64	15^{h}50^{m}35^s.2692	+05°27′10″.4484	13	Q	F	1.422	White et al. (1988)
1606+106	4C +10.45	16^{h}08^{m}46^s.2032	+10°29′07″.7758	13	Q	F	1.226	Stickel & Kühr (1994b)
1611+343	DA 406	16^{h}13^{m}41^s.0642	+34°12′47″.9089	23	Q	F	1.397	Adelman-McCarthy et al. (2007)
1633+382	4C +38.41	16^{h}35^{m}15^s.4930	+38°08′04″.5006	28	Q	F	1.814	Abazajian et al. (2005)
1637+574	OS 562	16^{h}38^{m}13^s.4563	+57°20′23″.9790	13	Q	F	0.751	Marziani et al. (1996)
1638+398	NRAO 512	16^{h}40^{m}29^s.6328	+39°46′46″.0285	16	Q	F	1.666	Stickel et al. (1989)
1641+399	3C 345	16^{h}42^{m}58^s.8100	+39°48′36″.9940	39	Q	F	0.593	Marziani et al. (1996)
1655+077	⋯	16^{h}58^{m}09^s.0115	+07°41′27″.5405	14	Q	F	0.621	Wilkes (1986)
1726+455	⋯	17^{h}27^{m}27^s.6508	+45°30′39″.7313	5	Q	F	0.717	Henstock et al. (1997)
1730−130	NRAO 530	17^{h}33^{m}02^s.7058	−13°04′49″.5483	16	Q	F	0.902	Junkkarinen (1984)
1739+522	4C +51.37	17^{h}40^{m}36^s.9778	+52°11′43″.4074	19	Q	F	1.379	Walsh et al. (1984)
1741−038	⋯	17^{h}43^{m}58^s.8561	−03°50′04″.6167	12	Q	F	1.054	White et al. (1988)
1749+096	OT 081	17^{h}51^{m}32^s.8186	+09°39′00″.7284	53	B[a]	F	0.322	Stickel et al. (1988)
1751+288	⋯	17^{h}53^{m}42^s.4736	+28°48′04″.9388	6	Q[d]	F	1.118	Healey et al. (2008)
1758+388	⋯	18^{h}00^{m}24^s.7654	+38°48′30″.6975	11	Q	F	2.092	Stickel & Kühr (1994a)
1800+440	⋯	18^{h}01^{m}32^s.3148	+44°04′21″.9002	12	Q	F	0.663	Walsh & Carswell (1982)
1803+784	⋯	18^{h}00^{m}45^s.6839	+78°28′04″.0184	32	B[a]	F	0.680	Rector & Stocke (2001)
1807+698	3C 371	18^{h}06^{m}50^s.6806	+69°49′28″.1085	21	B	F	0.051	de Grijp et al. (1992)
1823+568	4C +56.27	18^{h}24^{m}07^s.0684	+56°51′01″.4908	41	B[a]	F	0.664	Lawrence et al. (1986)
1828+487	3C 380	18^{h}29^{m}31^s.7809	+48°44′46″.1608	12	Q	S[e]	0.692	Lawrence et al. (1996)
1849+670	⋯	18^{h}49^{m}16^s.0723	+67°05′41″.6803	8	Q	F	0.657	Stickel & Kühr (1993a)
1928+738	4C +73.18	19^{h}27^{m}48^s.4952	+73°58′01″.5698	33	Q	F	0.302	Marziani et al. (1996)
1936−155	⋯	19^{h}39^{m}26^s.6577	−15°25′43″.0585	8	Q	F	1.657	Jauncey et al. (1984)
1957+405	Cygnus A	19^{h}59^{m}28^s.3565	+40°44′02″.0968	21	G	S	0.0561	Owen et al. (1997)
1958−179	⋯	20^{h}00^{m}57^s.0904	−17°48′57″.6726	8	Q	F	0.650	Browne et al. (1975)
2005+403	⋯	20^{h}07^{m}44^s.9448	+40°29′48″.6041	19	Q	F	1.736	Boksenberg et al. (1976)
2008−159	⋯	20^{h}11^{m}15^s.7109	−15°46′40″.2537	7	Q	F	1.180	Peterson et al. (1979)
2021+317	4C +31.56	20^{h}23^{m}19^s.0173	+31°53′02″.3061	12	U[d]	F	⋯	⋯
2021+614	OW 637	20^{h}22^{m}06^s.6818	+61°36′58″.8050	18	G	F	0.227	Hewitt & Burbidge (1991)
2037+511	3C 418	20^{h}38^{m}37^s.0347	+51°19′12″.6626	5	Q	F	1.686	Spinrad et al. (1985)
2121+053	⋯	21^{h}23^{m}44^s.5174	+05°35′22″.0931	10	Q	F	1.941	Steidel & Sargent (1991)
2128−123	⋯	21^{h}31^{m}35^s.2618	−12°07′04″.7960	10	Q	F	0.501	Searle & Bolton (1968)
2131−021	4C −02.81	21^{h}34^{m}10^s.3096	−01°53′17″.2387	17	B[a]	F	1.285	Drinkwater et al. (1997)
2134+004	⋯	21^{h}36^{m}38^s.5863	+00°41′54″.2128	30	Q	F	1.932	Osmer et al. (1994)
2136+141	OX 161	21^{h}39^{m}01^s.3093	+14°23′35″.9922	14	Q	F	2.427	Wills & Wills (1974)
2145+067	4C +06.69	21^{h}48^{m}05^s.4587	+06°57′38″.6042	17	Q	F	0.990	Steidel & Sargent (1991)
2155−152	⋯	21^{h}58^{m}06^s.2819	−15°01′09″.3277	12	Q	F	0.672	White et al. (1988)
2200+420	BL Lac	22^{h}02^{m}43^s.2914	+42°16′39″.9799	63	B	F	0.0686	Vermeulen et al. (1995)
2201+171	⋯	22^{h}03^{m}26^s.8937	+17°25′48″.2477	7	Q	F	1.076	Smith et al. (1977)
2201+315	4C +31.63	22^{h}03^{m}14^s.9758	+31°45′38″.2700	15	Q	F	0.295	Marziani et al. (1996)
2209+236	⋯	22^{h}12^{m}05^s.9663	+23°55′40″.5439	11	Q	F	1.125	Sowards-Emmerd et al. (2003)

Table 1
(Continued)

Source (1)	Alias (2)	R.A. (3)	Decl. (4)	N (5)	Opt. Cl. (6)	Radio (7)	z (8)	Reference for z (9)
2216−038	⋯	22^{h}18^{m}52^s.0377	−03°35′36″.8795	8	Q	F	0.901	Lynds (1967)
2223−052	3C 446	22^{h}25^{m}47^s.2593	−04°57′01″.3908	23	Q	F	1.404	Wright et al. (1983)
2227−088	PHL 5225	22^{h}29^{m}40^s.0843	−08°32′54″.4354	9	Q	F	1.560	Abazajian et al. (2004)
2230+114	CTA 102	22^{h}32^{m}36^s.4089	+11°43′50″.9041	24	Q	F	1.037	Falomo et al. (1994)
2243−123	⋯	22^{h}46^{m}18^s.2320	−12°06′51″.2775	11	Q	F	0.632	Browne et al. (1975)
2251+158	3C 454.3	22^{h}53^{m}57^s.7479	+16°08′53″.5609	53	Q	F	0.859	Jackson & Browne (1991)
2331+073	⋯	23^{h}34^{m}12^s.8282	+07°36′27″.5510	6	Q[d]	F	0.401	Sowards-Emmerd et al. (2005)
2345−167	⋯	23^{h}48^{m}02^s.6085	−16°31′12″.0223	12	Q	F	0.576	Tadhunter et al. (1993)
2351+456	4C +45.51	23^{h}54^{m}21^s.6802	+45°53′04″.2365	8	Q	F	1.986	Lawrence et al. (1996)

Columns are as follows: (1) IAU Name (B1950.0); (2) alternate name; (3) Right Ascension (J2000); (4) declination (J2000); (5) number of 15 GHz VLBA epochs analyzed; (6) optical classification according to the Véron-Cetty & Véron (2006) catalog (with exceptions as noted), where Q = quasar, B = BL Lac object, G = active galaxy, and U = unidentified; (7) description of radio spectrum from Kellermann et al. (2004), where F = flat, S = steep, and P = peaked; (8) redshift; (9) literature reference for redshift.

[a] Source classified as a quasar in the Véron-Cetty & Véron (2006) catalog.
[b] Source classified as a possible BL Lac object in the Véron-Cetty & Véron (2006) catalog.
[c] Source classified as a galaxy in the Véron-Cetty & Véron (2006) catalog.
[d] Source not listed in the Véron-Cetty & Véron (2006) catalog.
[e] Compact steep spectrum source.
(This table is available in machine-readable and Virtual Observatory (VO) forms in the online journal.)

3. OBSERVATIONS AND DATA REDUCTION

The 15 GHz VLBA data presented in this paper consist of observations carried out between 1994 and 2007 as part of the VLBA 2 cm Survey and MOJAVE programs, and data from the online NRAO data archive[13] spanning the period 1998–2006. The multi-epoch observations for each source, along with the corresponding image parameters, are described in Table 2. The 2 cm Survey observations analyzed by Kellermann et al. (2004) and E. Ros et al. (2009, in preparation) consist of approximately 1 hr integrations on each source, broken up into approximately 5 minute long scans separated in hour angle to improve (u, v) plane coverage. A similar observing method and integration times were used in the MOJAVE observations from 2002 May to 2007 September (VLBA codes BL111, BL123, BL137, and BL149; as flagged in Table 2), and are described in Paper I. During 2006 (VLBA codes BL137), the 15 GHz integration times were shortened by a factor of ∼3 to accommodate interleaved scans at three other observing frequencies (8.1, 8.4, and 12.1 GHz). The MOJAVE and 2 cm Survey observations were recorded at a data rate of 128 Mbps, which was increased to 256 Mbps in the epoch 2007 July 3 and epochs thereafter. Beginning with the 2007 January 6 epoch, the number of sources observed in each 24 hr MOJAVE session was increased from 18 to 25 sources to accommodate our larger monitoring sample (see Section 4.3).

In order to obtain the best possible temporal coverage to study jet kinematics, we re-analyzed all past VLBA 15 GHz observations that were available in the VLBA archive from 1998 to 2006 with good interferometric data on the sources in our sample. Since we require good (u, v) coverage to track jet motions accurately, we only considered the observations in which there were at least three scans on the source, suitably separated in hour angle. We also omitted any archival observations that had fewer than eight VLBA antennas. Any observations which lacked data from either of the outermost antennas (Mauna Kea and St. Croix) were also omitted if they had fewer than six scans on the remaining antennas. Finally,

we excluded a few archival epochs on some sources after processing them if their overall data quality was very poor due to weather and/or technical problems. Further details on these archival epochs can be obtained from the NRAO data archive using the appropriate VLBA code and observation date listed in Table 2.

Including the MOJAVE and 2 cm Survey epochs, we analyzed a total of 416 VLBA experiments, yielding 2424 individual source epochs on the MOJAVE sample. A portion of these were re-analyzed and/or presented in earlier 2 cm Survey and MOJAVE papers. We present the entire set of source epochs here for completeness.

The temporal coverage per source varies between 5 and 89 epochs, with a median of 15 epochs (Column (5) of Table 1). The wide dispersion reflects the fact that some AGNs are observed much more frequently with the VLBA, either as calibrators, or because they are sources of particular astrophysical interest. Also, attempts are made in the 2 cm Survey and MOJAVE programs to observe the sources with the most rapid motions more frequently, given the constraints associated with VLBA's dynamical scheduling system. In setting the observing intervals, we have aimed to not let the jet features move more than about half of their typical angular spacing between epochs. This is done to facilitate the unambiguous identification of the same features from one epoch to the next.

3.1. Data Reduction

We processed the data according to the standard procedures described in the AIPS cookbook.[14] Our overall reduction method was to initially flag out bad data on the basis of excessively high system temperature (typically due to inclement weather), remove sampler bias with the task ACCOR, calibrate the correlator output using antenna system temperature and gain curves, and apply an atmospheric opacity correction with APCAL. The pulse calibration signals were used in all the experiments to align the phases across the intermediate frequencies (IFs). In a few cases where no pulse calibration signal was

---

[13] http://archive.cv.nrao.edu/

[14] http://www.aips.nrao.edu

Table 2
Summary of 15 GHz Image Parameters

Source (1)	Epoch (2)	VLBA Code (3)	Frequency (GHz) (4)	B_{maj} (mas) (5)	B_{min} (mas) (6)	B_{pa} (°) (7)	I_{tot} (Jy) (8)	rms (mJy bm^{-1}) (9)	I_{base} (mJy bm^{-1}) (10)	Fig. Num.
0003−066	1995 Jul 28	BZ014[b]	15.3	1.17	0.51	0	2.172	0.5	3.0	1.1
	1996 Oct 27	BK37D[b]	15.4	1.20	0.45	−7	1.893	0.4	0.6	1.2
	1998 Oct 30	BK52D[b]	15.4	1.36	0.44	−14	2.642	0.4	1.5	1.3
	1999 Jun 17	BG091	15.4	1.36	0.53	−9	2.707	0.6	1.4	1.4
	2000 Jan 11	BK68D[b]	15.4	1.83	0.50	−14	2.431	0.3	4.4	1.5
	2001 Jan 21	BK68H[b]	15.4	1.62	0.58	−12	1.878	0.3	0.9	1.6
	2001 Oct 31	BR77A[b]	15.4	1.59	0.52	−12	1.559	0.2	1.4	1.7
	2002 May 19	BG121A	15.3	1.47	0.57	−8	2.192	0.5	1.2	1.8
	2003 Feb 5	BL111E[a]	15.4	1.32	0.53	−6	2.847	0.2	0.7	1.9
	2004 Mar 22	BG144A	15.4	1.34	0.54	−3	3.224	0.5	1.8	1.10
	2004 Jun 11	BL111M[a]	15.4	1.30	0.49	−7	3.302	0.3	1.5	1.11
	2005 Mar 23	BL123D[a]	15.4	1.33	0.53	−5	3.034	0.3	0.9	1.12
	2005 Jun 3	BL123H[a]	15.4	1.37	0.53	−8	3.017	0.2	0.9	1.13
	2005 Sep 16	BL123M[a]	15.4	1.33	0.52	−6	2.718	0.2	0.5	1.14

Columns are as follows: (1) IAU Name (B1950.0); (2) date of VLBA observation; (3) VLBA experiment code; (4) observing frequency in GHz; (5) FWHM major axis of restoring beam (milliarcseconds); (6) FWHM minor axis of restoring beam (milliarcseconds); (7) position angle of major axis of restoring beam; (8) total I flux density (Jy); (9) rms noise level of image (mJy per beam); (10) lowest I contour (mJy per beam); (11) figure number.
[a] Full polarization MOJAVE VLBA epoch.
[b] 2 cm VLBA Survey epoch.
(This table is available in its entirety in machine-readable and Virtual Observatory (VO) forms in the online journal. A portion is shown here for guidance regarding its form and content.)

available, we performed a fringe fit of a single scan on a bright calibrator and used the result to align the delays for the other sources. In the case of the archival epochs, and for MOJAVE epochs observed after 2007 August 9, we deemed the standard global fringe-fitting step to be unnecessary because of the strong and compact nature of all the sources, their well determined sky positions (e.g., from the ICRF, RDV, and VCS surveys, e.g., Fey et al. 2004; Petrov et al. 2008), and the well determined positions of the VLBA antennas. After a final bandpass correction and a short (30 s) phase self-calibration using a point-source model, we exported the data to Difmap (Shepherd 1997). The imaging and self-calibration process in Difmap was largely automated, with human input required mainly for data flagging. The procedure was facilitated by the use of a *mySQL* database containing the locations of clean boxes for each source, which we determined during the processing of previous epochs. Since the overall extent of the individual sources did not significantly vary over the time period covered by our survey, the use of pre-determined clean boxes provided additional a priori information that guided the self-calibration process and facilitated rapid convergence toward the final model. For experiments in which polarimetric cross-hand data were recorded, we performed additional calibration steps to correct for antenna leakage terms and the absolute electric vector position angle on the sky, as described in Paper I. These multi-epoch polarization data will be presented in a separate paper.

3.2. Images

We produced the final images using Difmap with a multiresolution clean algorithm developed by Moellenbrock (1998). The technique involves "super resolving" the brightest and most compact features in the initial cleaning stages, which leads to a more accurate representation of lower surface brightness features in the final (natural weighted) cleaning stages. The final step consisted of a large iteration deep clean, which also helps bring out these features. This procedure does, however, alter the

noise statistics in the final cleaned image. For this reason we obtained the rms image noise values from a blank sky region a full arcsecond away from the CLEAN image center after the final cleaning stage. This provided a better estimate of the true rms image noise associated with the interferometric visibilities, since this region was located well outside the deep CLEAN box of the main image.

We present the untapered, naturally weighted images of all the individual source epochs in Figure 1. The dimensions of the restoring beam in each image vary depending on the (u, v) coverage of the individual observation. Information on the restoring beam can be found in Table 2, along with the lowest contour level, VLBA experiment code, and observation date. The image dynamic range varies with (u, v) coverage and integration time, with typical values of approximately 5000:1. We obtained the total flux densities by summing all emission from pixels in the image above the lowest contour level within the region shown in Figure 1. Gaussian model fits to the visibility data, as well as a kinematic analysis of the sample, will be presented in a separate paper.

In order to show the fullest possible extent of the jets, we have also produced "stacked" naturally and uniformly weighted images of each source (Figure 2). We created the former by first restoring the image at each epoch with an identical beam whose dimensions corresponded to the median naturally weighted beam of all epochs on that source. We then shifted the convolved image at each epoch to align the fitted positions of the core features, and then combined them all with equal weight to produce an averaged (stacked) image. We created the uniformly weighted images in the same manner, using a restoring beam that was 80% of the naturally weighted beam size in both dimensions.

We note that in the case of a few sources located within $\sim 1°.5$ of the celestial equator, the individual baseline tracks in the (u, v) plane are almost exclusively in the east–west direction, resulting in relatively poorer interferometric coverage.
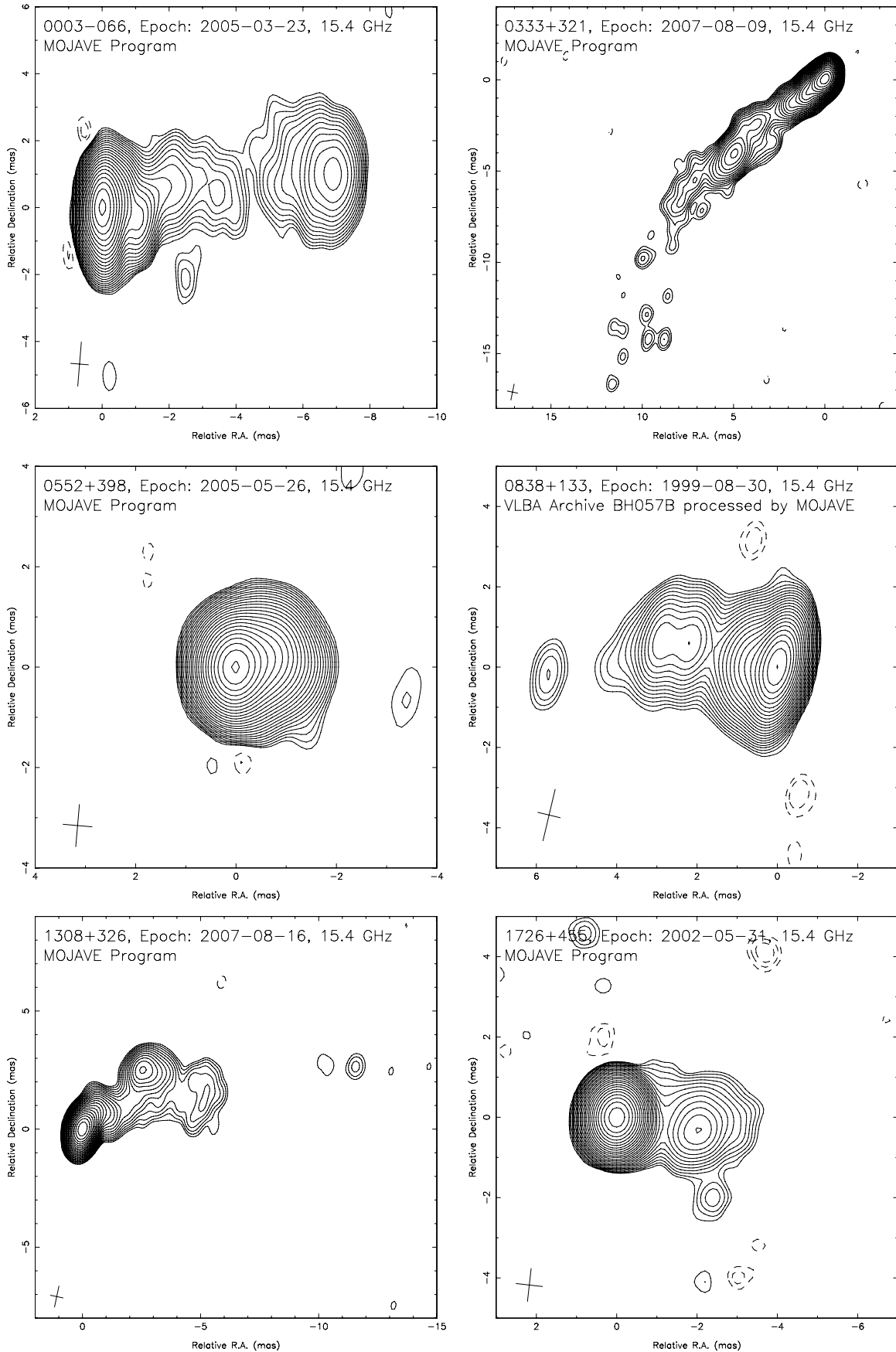
Figure 1. Naturally weighted 15 GHz total intensity VLBA contour images of individual epoch observations of the MOJAVE AGN sample. The contours are in successive powers of $\sqrt{2}$ times the base contour level given in Table 2. Because of self-calibration, in some cases the origin may be coincident with the brightest feature in the image, rather than the putative core component. Clockwise from the top left: image of 0003−066, 0333+321, 0838+133, 1726+455, 1308+326, 0552+398.

(An extended version of this figure is available in the online journal.)
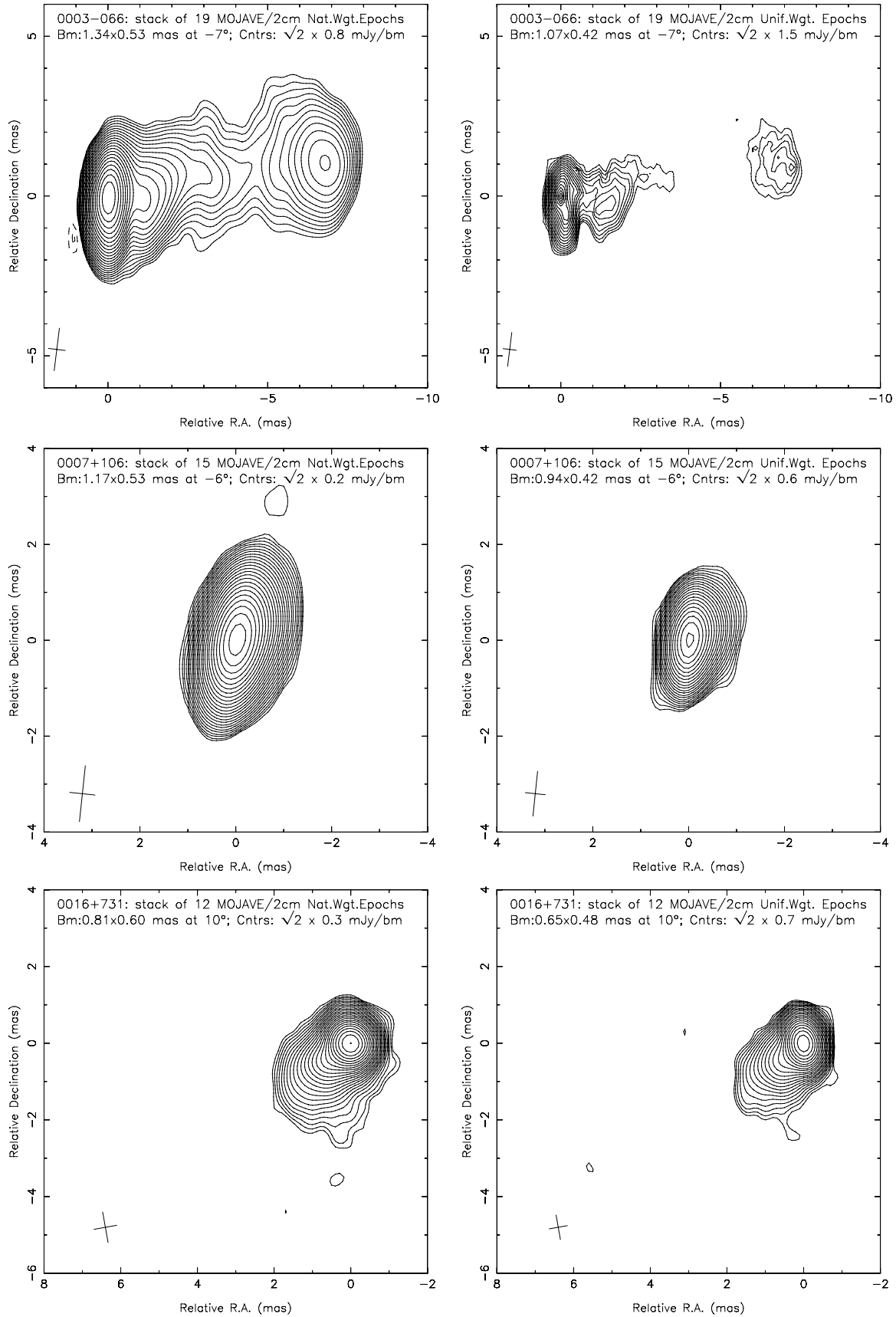
Figure 2. Total intensity 15 GHz VLBA stacked-epoch contour images of the MOJAVE AGN sample. The left-hand panels represent the unweighted averages of the naturally weighted images presented in Figure 1, after shifting each map to make the core component coincident with the origin. The right-hand panels contain stacked uniformly weighted images with beam dimensions 80% of the naturally weighted images. From top to bottom are stacked images of 0003−066, 0007+106, and 0016+731.

(An extended version of this figure is available in the online journal.)

This can create artifacts to the direct north and south of the brightest feature, as seen in some of the stacked and individual epoch images (e.g., 1055+018, 2134+004). VLBA images of equatorial sources with jets aligned in the north and south directions on the sky suffer particularly from this effect.

A very small number of our images may also suffer from the effects of rapid intraday variability (IDV). Since the imaging procedure assumes that the source flux density is not significantly changing on the (several hour long) timescale of the observation, intrinsic source variability can add error to the gain solutions, with a resulting increase in image noise. We have discovered one such case in 1156+295, epoch 2007 February 5 (Savolainen & Kovalev 2008). We are currently analyzing our whole data set for other instances of IDV (H. S. Kuchibhotla et al. 2009, in preparation).

The full set of all images is included in the online version of this article. Linearly interpolated movies which show the jet motions and structural variability, FITS images, and calibrated visibility data are also publicly available on the MOJAVE Web site.[15] The images presented in this paper cover epochs up to the end of 2007. More recent images and calibrated visibility data from our current program are uploaded to the Web site as soon as they are reduced, typically 3–4 weeks after each observing session. All of the raw visibility data associated with the MOJAVE program are publicly available immediately after correlation from the NRAO data archive.

4. MORPHOLOGY

The appearance of blazar jets depends not only on their intrinsic structure but also on the Doppler factor associated with the highly relativistic motion of individual features in the jet. Their small viewing angles can highly exaggerate mild curvatures in the jet flow, and relativistic beaming effects can amplify or diminish the apparent brightness of different jet regions as the result of even minor changes in the direction of motion with respect to the LOS. It is thought that all jets must be intrinsically double-sided to explain the transport of energy from the central engine to the double radio lobes commonly found in FRI and FRII radio galaxies and in some quasars. In many cases, however, the visible morphology of these jets is highly affected by differential Doppler boosting. The apparent flux density ratio of the approaching and receding jets may reach as high as 10^6 in the fastest known jets, giving the illusion of a one-sided jet in VLBI images made with limited sensitivity and dynamic range.

All but eight MOJAVE sources in our sample have the asymmetrical characteristics of one-sided jets, which is indicative of the high degree of relativistic beaming in the sample. Five sources have two-sided jets, of which four are low-luminosity AGNs (Section 4.2). A small number of such weakly beamed sources are expected to be present in our flux-density-limited sample, by virtue of their proximity. We note that earlier authors have speculated on the two-sided nature of the parsec-scale jet in the luminous radio galaxy 2021+614 (Tschager et al. 2000; Peck & Taylor 2000). However, since the southernmost feature is more variable, more compact (Lister 2001), and has a flat spectral index (Barvainis & Lonsdale 1998) as compared to the other jet features, we consider it as the core feature in a one-sided jet.

4.1. Unresolved and Nearly Unresolved Sources

We have found that three sources (0235+164, 1741−038, and 1751+288) are effectively unresolved by the VLBA at 15 GHz at all epochs, with essentially all of the flux density contained within a few tenths of a milliarcsecond. Model fitting of the visibility data for 0235+164 and 1741−038 indicated possible structure on a scale of $\sim$ 0.3 mas; however, we could not reliably cross-identify any components across multiple epochs for either of these sources. Another source, 1324+224, is mostly very compact, but has a very weak feature located approximately 3 mas to the southwest of the bright core feature. However, its measured position was erratic across multiple epochs and we were unable to define any meaningful motions in this source. The stacked-epoch image of 1739+522 contains a weak diffuse structure to the north of a prominent compact core, which may be part of a highly curved jet.

These sources could appear very compact either because their jets are atypically weak, or they possess a highly beamed core that swamps the jet emission in our limited sensitivity/dynamic range images. It is also possible that they may be experiencing a period of inactivity in which new jet components are not being ejected. We have witnessed the latter in 1308+326, which had very little discernible jet structure prior to 1997, and now has a pronounced mas-scale jet (Figure 1).

With the exception of 0235+164, none of the five compact sources mentioned above show significant extended radio structure in deep VLA images (Ulvestad et al. 1981; Perley et al. 1982; Cooper et al. 2007). They are therefore well suited as calibration sources for flux density and absolute polarization position angle calibration when simultaneous single-dish/VLA and VLBA data are available. Since any observable jet structure in these objects must be on angular scales just at or less than the size of the 2 cm VLBA restoring beam, their kinematics would be best studied with shorter wavelength ground and/or space VLBI, which can provide better spatial resolution.

4.2. Two-Sided Jets

Multi-epoch observations of two-sided AGN jets are extremely useful for testing whether apparent motions of jet features do indeed reflect the underlying flow. In the case of random pattern speeds, we would not necessarily expect motions in the jet and counter-jet to be correlated. Detailed kinematic studies of two-sided AGN jets (e.g., Taylor & Vermeulen 1997; Vermeulen et al. 2003) have revealed similar speeds in the jet and counter-jet, and have provided additional estimates of the viewing angles to these jets. In this section, we provide brief descriptions of the five two-sided AGN jets in the MOJAVE sample.

0238−084 (NGC 1052): the morphology and kinematics of this source have been studied extensively by Vermeulen et al. (2003). The jet shows numerous features moving outward along the jet and counter-jet at speeds up to $\sim$ 0.3c. Multifrequency VLBA observations by Vermeulen et al. (2003) and Kadler et al. (2004) indicate that the core feature is obscured at 15 GHz by strong free–free absorption associated with a circumnuclear torus. A more detailed analysis of the multi-epoch structure of NGC 1052 based on MOJAVE and additional 22 and 43 GHz data from a dedicated multiwavelength monitoring campaign is currently underway (E. Ros et al. 2009, in preparation).

0316+413 (3C 84, NGC 1275): although pre-VLBA observations indicated a one-sided jet, albeit with complex structure, the earliest 15 GHz VLBA observations revealed a previously undetected component which had been obscured at the lower

---

frequencies used previously. Extensive observations by Walker et al. (2000) have indicated that the northern lobe is likely being affected by free–free absorption from ionized gas associated with an accretion disk. The central feature contains complex substructure and motions (Dhawan et al. 1998), including several distinct circularly polarized regions seen in the MOJAVE data (Homan & Lister 2006) and at lower frequencies (Homan & Wardle 2004).

1228+126 (M87): the 15 GHz VLBA kinematics of this nearby AGN were reported by Kovalev et al. (2007), and consist of relatively slow speeds below $0.07c$. We have taken the core to be coincident with the brightest component, for which we have also detected circular polarization (Paper II); a faint counter-jet is observed not only at 2 cm (Kovalev et al. 2007) but also with higher resolution at 13 and 7 mm (Ly et al. 2007).

1413+135: this highly unusual two-sided BL Lac object with an apparent spiral host galaxy has been the subject of previous VLBI studies by Perlman et al. (1994, 1996, 2002) and Wiik et al. (2001). At 15 GHz, we see a mostly one-sided jet pointing toward the west, but at longer wavelengths there is a prominent but more diffuse jet pointing toward the east. The LOS to the nucleus shows H I and molecular absorption (Conway 1999). It is the only high-luminosity two-sided jet in the MOJAVE sample. Although 1413+135 has been classified as a compact symmetric object by Gugliucci et al. (2005), its core component is highly variable, which is not a general characteristic of that class.

1957+405 (Cygnus A): the parsec-scale jet of this nearby radio galaxy contains a number of well-defined features in both the main jet and the counter-jet. The jet kinematics have been studied by Bach et al. (2005), based in part on 2 cm VLBA survey and MOJAVE data, and their multifrequency VLBA analysis suggests that like NGC 1052 and 3C 84, the counter-jet is partially obscured by an absorbing torus.

Although it is tempting to interpret their morphology and absorption as evidence that these two-sided jets are plane-of-the-sky versions of the one-sided jets, Cohen et al. (2007) have demonstrated that the low-luminosity two-sided sources apparently do not differ from the high-luminosity one-sided sources solely because of their orientations. Kovalev et al. (2007) have also argued that the prominent parsec-scale jet in M87 may be intrinsically one-sided. The kinematic interpretation of the two-sided jets in the MOJAVE sample will be presented in a separate paper.

4.3. Current Monitoring Program and Additional Sources

The flux-density-limited MOJAVE sample is statistically complete on the basis of compact emission at 15 GHz, which is essential for understanding the complex selection biases associated with observed blazar samples. However, new high-energy observatories such as Fermi are likely to detect a broader range of blazars than those derived from a strictly radio-selected sample. For this reason, in 2006 we expanded the MOJAVE monitoring program beyond the flux-density-limited sample to encompass 65 additional sources of interest. These include (1) a subsample of lower-luminosity AGNs with 8 GHz VLBA flux density greater than 0.35 Jy, 8 GHz VLBA luminosity $< 10^{26}$ W Hz^{-1} and $z < 0.3$ that we identified using the VLBA Calibrator Survey (Beasley et al. 2002; Fomalont et al. 2003; Petrov et al. 2005), (2) several additional AGNs identified as high-confidence EGRET gamma-ray associations by Sowards-Emmerd et al. (2003, 2004), and (3) several AGNs known to have particularly interesting or unusual kinematics from our

prior 2 cm VLBA survey observations (Kellermann et al. 2004). The current AGN monitoring list can be found at the MOJAVE Web site.

As of Fall 2008, the MOJAVE program is regularly monitoring 200 AGNs with the VLBA at 15 GHz, the UMRAO 26 m radio telescope at 5, 8, and 15 GHz, and the RATAN 600 m telescope at 1, 2.3, 4.8, 7.7, 11, and 22 GHz. We anticipate adding up to 100 additional AGNs to our current monitoring list, based on new gamma-ray detections made by the Fermi LAT instrument (Abdo et al. 2009), provided these sources have sufficient compact flux density ($\gtrsim 100$ mJy) for imaging with the VLBA at 15 GHz. This extended sample will ensure complete coverage of several regions of the gamma-ray/radio flux density plane, and will be used for correlative studies.

5. SUMMARY

The MOJAVE program represents the largest full-polarization high-resolution monitoring program of powerful AGN jets carried out to date. The complete flux-density-limited sample of 135 sources contains the brightest and most highly beamed AGNs visible in the northern sky. Composed primarily of blazars, it is especially useful for comparisons with studies at other wavelengths, especially at very high energies, where blazars tend to dominate the all-sky catalogs. In 2006, we expanded the monitoring sample to include 65 additional AGNs on the basis of their known gamma-ray emission, low luminosity, and/or unusual jet kinematics. This list will be further supplemented with new AGN detections from the Fermi gamma-ray observatory.

By combining archival data from the 2 cm Survey and other VLBA programs, we have obtained 2424 individual 15 GHz VLBA images on the flux-density-limited MOJAVE sample, covering the period 1994 August to 2007 September. The full set of images is publicly available on the MOJAVE Web site. These data indicate that 94% of the jets are one-sided, likely due to relativistic beaming effects. Of the remainder, three AGNs (0235+164, 1741−038, and 1751+288) are essentially unresolved on VLBA scales, having essentially all of their flux density contained within a few tenths of a milliarcsecond. Five other AGNs: 0238-084(NGC 1052), 0316+413 (3C 84), 1228+126 (M87), 1413+135, 1957+405 (Cygnus A), have two-sided jet morphologies. The statistical and kinematic analysis of the full data set will be presented in subsequent papers in this series.

REFERENCES

Abazajian, K., et al. 2004, AJ, 128, 502
Abazajian, K., et al. 2005, AJ, 129, 1755
Abdo, A. A., et al. 2009, ApJS, submitted, arXiv:0902.1340
Adelman-McCarthy, J., et al. 2006, ApJS, 162, 38
Adelman-McCarthy, J., et al. 2007, ApJS, 172, 634
Akiyama, M., Ueda, Y., Ohta, K., Takahashi, T., & Yamada, T. 2003, ApJS, 148, 275
Aldcroft, T. L., Bechtold, J., & Elvis, M. 1994, ApJS, 93, 1
Aller, M. F., Aller, H. D., & Hughes, P. A. 1992, ApJ, 399, 16
Bach, U., Kadler, M., Krichbaum, T. P., Middelberg, E., Alef, W., Witzel, A., & Zensus, J. A. 2005, in ASP Conf. Proc. 340, Future Directions in High Resolution Astronomy, ed. J. Romney & M. Reid (San Francisco, CA: ASP), 30
Barvainis, R., & Lonsdale, C. 1998, AJ, 115, 885
Beasley, A. J., Gordon, D., Peck, A. B., Petrov, L., MacMillan, D. S., Fomalont, E. B., & Ma, C. 2002, ApJS, 141, 13
Best, P. N., Peacock, J. A., Brookes, M. H., Dowsett, R. E., Röttgering, H. J. A., Dunlop, J. S., & Lehnert, M. D. 2003, MNRAS, 346, 1021
Boisse, P., & Bergeron, J. 1988, A&A, 192, 1
Boksenberg, A., Briggs, S. A., Carswell, R. F., Schmidt, M., & Walsh, D. 1976, MNRAS, 177, 43P
Britzen, S., et al. 2007, A&A, 472, 763
Britzen, S., et al. 2008, A&A, 484, 119
Browne, I. W. A., Savage, A., & Bolton, J. G. 1975, MNRAS, 173, 87P
Burbidge, E. M. 1970, ApJ, 160, L33
Cara, M., & Lister, M. L. 2008, ApJ, 674, 111 (Paper IV)
Carangelo, N., Falomo, R., Kotilainen, J., Treves, A., & Ulrich, M.-H. 2003, A&A, 412, 651
Cohen, M. H., Lister, M. L., Homan, D. C., Kadler, M., Kellermann, K. I., Kovalev, Y. Y., & Vermeulen, R. C. 2007, ApJ, 658, 232
Cohen, M. H., et al. 1975, ApJ, 201, 249
Cohen, M. H., et al. 1977, Nature, 268, 405
Cohen, R. D., Smith, H. E., Junkkarinen, V. T., & Burbidge, E. M. 1987, ApJ, 318, 577
Conway, J. E. 1999, New Astron. Rev., 43, 509
Cooper, N. J., Lister, M. L., & Kochanczyk, M. D. 2007, ApJS, 171, 376 (Paper III)
Croom, S. M., Smith, R. J., Boyle, B. J., Shanks, T., Miller, L., Outram, P. J., & Loaring, N. S. 2004, MNRAS, 349, 1397
de Grijp, M. H. K., Keel, W. C., Miley, G. K., Goudfrooij, P., & Lub, J. 1992, A&AS, 96, 389
Denicoló, G., Terlevich, R., Terlevich, E., Forbes, D. A., Terlevich, A., & Carrasco, L. 2005, MNRAS, 356, 1440
Dhawan, V., Kellermann, K. I., & Romney, J. D. 1998, ApJ, 498, L111
Drinkwater, M. J., et al. 1997, MNRAS, 284, 85
Eckart, A., Witzel, A., Biermann, P., Johnston, K. J., Simon, R., Schalinski, C., & Kuhr, H. 1986, A&A, 168, 17
Eracleous, M., & Halpern, J. P. 2004, ApJS, 150, 181
Falomo, R., Scarpa, R., & Bersanelli, M. 1994, ApJS, 93, 125
Fey, A. L., et al. 2004, AJ, 127, 3587
Fomalont, E., Petrov, L., McMillan, D. S., Gordon, D., & Ma, C. 2003, AJ, 126, 2562
Gordon, D., Petrov, L., Kovalev, Y. Y., & Fomalont, E. 2005, AJ, 129, 1163
Gugliucci, N. E., Taylor, G. B., Peck, A. B., & Giroletti, M. 2005, ApJ, 622, 136
Halpern, J. P., Eracleous, M., & Mattox, J. R. 2003, AJ, 125, 572
Hartman, R. C., et al. 1999, ApJS, 123, 79
Healey, S. E., et al. 2008, ApJS, 175, 97
Henstock, D. R., Browne, I. W. A., Wilkinson, P. N., & McMahon, R. G. 1997, MNRAS, 290, 380

Hewett, P. C., Foltz, C. B., & Chaffee, F. H. 1995, AJ, 109, 1498
Hewitt, A., & Burbidge, G. 1991, ApJS, 75, 297
Homan, D. C., & Lister, M. L. 2006, AJ, 131, 1262 (Paper II)
Homan, D. C., Lister, M. L., Kellermann, K. I., Cohen, M. H., Ros, E., Zensus, J. A., Kadler, M., & Vermeulen, R. C. 2003, ApJ, 589, L9
Homan, D. C., & Wardle, J. F. C. 2004, ApJ, 602, L13
Homan, D. C., et al. 2006, ApJ, 642, L115
Hook, I. M., McMahon, R. G., Irwin, M. J., & Hazard, C. 1996, MNRAS, 282, 1274
Hunstead, R. W., Murdoch, H. S., & Shobbrook, R. R. 1978, MNRAS, 185, 149
Hunter, S. D., et al. 1993, ApJ, 409, 134
Jackson, N., & Browne, I. W. A. 1991, MNRAS, 250, 414
Jauncey, D. L., Batty, M. J., Wright, A. E., Peterson, B. A., & Savage, A. 1984, ApJ, 286, 498
Jorstad, S. G., et al. 2007, AJ, 134, 799
Junkkarinen, V. 1984, PASP, 96, 539
Kadler, M., Ros, E., Lobanov, A. P., Falcke, H., & Zensus, J. A. 2004, A&A, 426, 481
Kadler, M., et al. 2008, ApJ, 680, 867
Kellermann, K. I., Vermeulen, R. C., Zensus, J. A., & Cohen, M. H. 1998, AJ, 115, 1295
Kellermann, K. I., et al. 2004, ApJ, 609, 539
Kovalev, Y. Y., Lister, M. L., Homan, D. C., & Kellermann, K. I. 2007, ApJ, 668, L27
Kovalev, Y. Y., Nizhelsky, N. A., Kovalev, Yu. A., Berlin, A. B., Zhekanis, G. V., Mingaliev, M. G., & Bogdantsov, A. V. 1999, A&AS, 139, 545
Kovalev, Y. Y., et al. 2005, AJ, 130, 2473
Lawrence, C. R., Pearson, T. J., Readhead, A. C. S., & Unwin, S. C. 1986, AJ, 91, 494
Lawrence, C. R., Zucker, J. R., Readhead, A. C. S., Unwin, S. C., Pearson, T. J., & Xu, W. 1996, ApJS, 107, 541
Lister, M. L. 2001, ApJ, 562, 208
Lister, M. L., & Homan, D. C. 2005, AJ, 130, 1389 (Paper I)
Lister, M. L., Kellermann, K. I., Vermeulen, R. C., Cohen, M. H., Zensus, J. A., & Ros, E. 2003, ApJ, 584, 135
Lister, M. L., & Marscher, A. P. 1997, ApJ, 476, 572
Ly, C., Walker, R. C., & Junor, W. 2007, ApJ, 660, 200
Lynds, C. R. 1967, ApJ, 147, 837
Marziani, P., Sulentic, J. W., Dultzin-Hacyan, D., Calvani, M., & Moles, M. 1996, ApJS, 104, 37
McIntosh, D. H., Rieke, M. J., Rix, H.-W., Foltz, C. B., & Weymann, R. J. 1999, ApJ, 514, 40
Michel, A., & Huchra, J. 1988, PASP, 100, 1423
Moellenbrock, G. 1998, PhD thesis, Brandeis Univ.
Nilsson, K., Pursimo, T., Sillanpää, A., Takalo, L. O., & Lindfors, E. 2008, A&A, 487, L29
Osmer, P. S., Porter, A. C., & Green, R. F. 1994, ApJ, 436, 678
Osterbrock, D. E., & Pogge, R. W. 1987, ApJ, 323, 108
Owen, F. N., Ledlow, M. J., Morrison, G. E., & Hill, J. M. 1997, ApJ, 488, L15
Peck, A. B., & Taylor, G. B. 2000, ApJ, 534, 90
Perley, R. A., Fomalont, E. B., & Johnston, K. J. 1982, ApJ, 255, L93
Perlman, E. S., Carilli, C. L., Stocke, J. T., & Conway, J. 1996, AJ, 111, 1839
Perlman, E. S., Padovani, P., Giommi, P., Sambruna, R., Jones, L. R., Tzioumis, A., & Reynolds, J. 1998, AJ, 115, 1253
Perlman, E. S., Stocke, J. T., Carilli, C. L., Sugiho, M., Tashiro, M., Madejski, G., Wang, Q. D., & Conway, J. 2002, AJ, 124, 2401
Perlman, E. S., Stocke, J. T., Shaffer, D. B., Carilli, C. L., & Ma, C. 1994, ApJ, 424, L69
Peterson, B. A., Wright, A. E., Jauncey, D. L., & Condon, J. J. 1979, ApJ, 232, 400
Petrov, L., Kovalev, Y. Y., Fomalont, E., & Gordon, D. 2008, AJ, 136, 580
Piner, B. G., Mahmud, M., Fey, A. L., & Gospodinova, K. 2007, AJ, 133, 2357
Rector, T. A., & Stocke, J. T. 2001, AJ, 122, 565
Sargent, W. L. W. 1970, ApJ, 160, 405
Savolainen, T., & Kovalev, Y. Y. 2008, A&A, 489, L33
Sbarufatti, B., Treves, A., Falomo, R., Heidt, J., Kotilainen, J., & Scarpa, R. 2005, AJ, 129, 559
Schilizzi, R. T., Cohen, M. H., Shaffer, D. B., Kellermann, K. I., Swenson, G. W., Jr., Yen, J. L., Rinehart, R., & Romney, J. D. 1975, ApJ, 201, 263
Schmidt, M. 1977, ApJ, 217, 358
Searle, L., & Bolton, J. G. 1968, ApJ, 154, L101
Shaffer, D. B., Cohen, M. H., Schilizzi, R. T., Kellermann, K. I., Swenson, G. W., Jr., Yen, J. L., Rinehart, R., & Romney, J. D. 1975, ApJ, 201, 256
Shepherd, M. C. 1997, in ASP Conf. Proc. 125, Astronomical Data Analysis Software and Systems VI, ed. G. Hunt & H. E. Payne (San Francisco, CA: ASP) 77

Smith, H. E., Burbidge, E. M., Baldwin, J. A., Tohline, J. E., Wampler, E. J., Hazard, C., & Murdoch, H. S. 1977, ApJ, 215, 427

Smith, R. J., Lucey, J. R., Hudson, M. J., Schlegel, D. J., & Davies, R. L. 2000, MNRAS, 313, 469

Sowards-Emmerd, D., Romani, R. W., & Michelson, P. F. 2003, ApJ, 590, 109

Sowards-Emmerd, D., Romani, R. W., Michelson, P. F., Healey, S. E., & Nolan, P. L. 2005, ApJ, 626, 95

Sowards-Emmerd, D., Romani, R. W., Michelson, P. F., & Ulvestad, J. S. 2004, ApJ, 609, 564

Spinrad, H., Marr, J., Aguilar, L., & Djorgovski, S. 1985, PASP, 97, 932

Steidel, C. C., & Sargent, W. L. W. 1991, ApJ, 382, 433

Stickel, M., Fried, J. W., & Kühr, H. 1988, A&A, 191, L16

Stickel, M., Fried, J. W., & Kühr, H. 1989, A&AS, 80, 103

Stickel, M., Fried, J. W., & Kühr, H. 1993, A&AS, 98, 393

Stickel, M., Fried, J. W., Kühr, H., Padovani, P., & Urry, C. M. 1991, ApJ, 374, 431

Stickel, M., & Kühr, H. 1993a, A&AS, 100, 395

Stickel, M., & Kühr, H. 1993b, A&AS, 101, 521

Stickel, M., & Kühr, H. 1994a, A&AS, 103, 349

Stickel, M., & Kühr, H. 1994b, A&AS, 105, 67

Stickel, M., Kühr, H., & Fried, J. W. 1993, A&AS, 97, 483

Stickel, M., Meisenheimer, K., & Kühr, H. 1994, A&AS, 105, 211

Strauss, M. A., Huchra, J. P., Davis, M., Yahil, A., Fisher, K. B., & Tonry, J. 1992, ApJS, 83, 29

Strittmatter, P. A., Carswell, R. F., Gilbert, G., & Burbidge, E. M. 1974, ApJ, 190, 509

di Tadhunter, C. N., Morganti, R., Serego-Alighieri, S., Fosbury, R. A. E., & Danziger, I. J. 1993, MNRAS, 263, 999

Taylor, G. B., & Vermeulen, R. C. 1997, ApJ, 485, L9

Thompson, D. J. 2004, New Astron. Rev., 48, 543

Thompson, D. J., Djorgovski, S., & de Carvalho, R. 1990, PASP, 102, 1235

Torniainen, I., Tornikoski, M., Teräsranta, H., Aller, M. F., & Aller, H. D. 2005, A&A, 435, 839

Tschager, W., Schilizzi, R. T., Röttgering, H. J. A., Snellen, I. A. G., & Miley, G. K. 2000, A&A, 360, 887

Tytler, D., & Fan, X.-M. 1992, ApJS, 79, 1

Ulvestad, J., Johnston, K., Perley, R., & Fomalont, E. 1981, AJ, 86, 1010

Vermeulen, R. C., Ogle, P. M., Tran, H. D., Browne, I. W. A., Cohen, M. H., Readhead, A. C. S., Taylor, G. B., & Goodrich, R. W. 1995, ApJ, 452, L5

Vermeulen, R. C., Ros, E., Kellermann, K. I., Cohen, M. H., Zensus, J. A., & van Langevelde, H. J. 2003, A&A, 401, 113

Veron-Cetty, M.-P., & Veron, P. 1989, Eur. South. Obs. Sci. Rep., 7, 1

Véron-Cetty, M.-P., & Véron, P. 2006, A&A, 455, 773

Walker, R. C., Dhawan, V., Romney, J. D., Kellermann, K. I., & Vermeulen, R. C. 2000, ApJ, 530, 233

Walsh, D., Beckers, J. M., Carswell, R. F., & Weymann, R. J. 1984, MNRAS, 211, 105

Walsh, D., & Carswell, R. F. 1982, MNRAS, 200, 191

White, G. L., Jauncey, D. L., Wright, A. E., Batty, M. J., Savage, A., Peterson, B. A., & Gulkis, S. 1988, ApJ, 327, 561

Wiik, K., Valtaoja, E., & Leppänen, K. 2001, A&A, 380, 72

Wiklind, T., & Combes, F. 1997, A&A, 328, 48

Wilkes, B. J. 1986, MNRAS, 218, 331

Wills, D., & Lynds, R. 1978, ApJS, 36, 317

Wills, D., & Wills, B. J. 1974, ApJ, 190, 271

Wright, A. E., Ables, J. G., & Allen, D. A. 1983, MNRAS, 205, 793

Zensus, A., Ros, E., Kellermann, K. I., Cohen, M. H., & Vermeulen, R. C. 2002, AJ, 124, 662

Zensus, J. A., Cohen, M. H., & Unwin, S. C. 1995, ApJ, 443, 35